Extreme storms cause rapid but short-lived shifts in nearshore subtropical bacterial communities

Ángela Ares[1*], Margaret Mars Brisbin[1*], Kirk N. Sato[1,2], Juan P. Martín[1], Yoshiteru Iinuma[3], Satoshi Mitarai[1]

* contributed equally

[1] Marine Biophysics Unit, Okinawa Institute of Science and Technology (OIST, Okinawa, Japan)

[2] Friday Harbor Laboratories, University of Washington (U.S.A.)

[3] Instrumental Analysis Section, Okinawa Institute of Science and Technology (OIST, Okinawa, Japan)

Originality-Significance Statement

Extreme storm events, such as tropical cyclones, can negatively affect coastal ecosystems through increased terrestrial run-off, pollution, and physical destruction. Future climate scenarios predict increased frequency and intensity of tropical cyclones, necessitating a better understanding of how ecosystems respond to such events. In this study, we show the short-term dynamics of nearshore bacterial communities during two major tropical cyclones occurring at the beginning and end of the typhoon season in the subtropical western Pacific. Importantly, field observations were coupled with concurrent mesocosm experiments to isolate the effects of terrestrial sediment input from other storm effects, such as wind, waves, and fresh-water influx. Our study reveals that shifts in bacterial communities in both instances were extremely rapid but highly context dependent.

Abstract

Climate change scenarios predict tropical cyclones will increase in both frequency and intensity, which will escalate the amount of terrestrial run-off and mechanical disruption affecting coastal ecosystems. Bacteria are key contributors to ecosystem functioning, but relatively little is known

about how they respond to extreme storm events, particularly in nearshore subtropical regions. In this study, we combine field observations and mesocosm experiments to assess bacterial community dynamics and changes in physicochemical properties during early- and late-season tropical cyclones affecting Okinawa, Japan. Storms caused large and fast influxes of freshwater and terrestrial sediment—locally known as red soil pollution—and caused moderate increases of macronutrients, especially SiO_2 and PO_4^{3-}, with up to 25 and 0.5 µM, respectively. We detected shifts in relative abundances of marine and terrestrially-derived bacteria, including putative coral and human pathogens, during storm events. Soil input alone did not substantially affect marine bacterial communities in mesocosms, indicating that other components of run-off or other storm effects likely exert a larger influence on bacterial communities. The storm effects were short-lived and bacterial communities quickly recovered following both storm events. The early- and late-season storms caused different physicochemical and bacterial community changes, demonstrating the context-dependency of extreme storm responses in a subtropical coastal ecosystem.

Keywords

Tropical cyclones, typhoons, hurricanes, extreme events, bacterioplankton, coastal, nearshore, community dynamics, soil pollution, run-off

Introduction

Extreme storm events, such as tropical cyclones (i.e. tropical storms, hurricanes, and typhoons), can have dramatic consequences on coastal ecosystems, due in part to the effects of terrestrially-derived pollution (Hennessy *et al.*, 1997; De Jesus Crespo *et al.*, 2019). In addition to influencing salinity and turbidity, flood plumes often include elevated concentrations of bacteria (Solo-Gabriele *et al.*, 2000), nutrients (i.e. C, N, P) (Chen *et al.*, 2012, 2018; Gao *et al.*,

2014; Paerl *et al.*, 2018) and other chemicals, such as herbicides or heavy metals (Lewis *et al.*, 2012; Mistri *et al.*, 2019), which can act synergistically to negatively affect coastal ecosystems (Wooldridge, 2009; Brodie *et al.*, 2012; Lewis *et al.*, 2012). Especially in tropical and subtropical regions experiencing severe seasonal storms, large volumes of terrestrial run-off entering coastal waters can degrade coastal ecosystems, including coral reefs, through sedimentation or disease (Riegl and Branch, 1995; Philipp and Fabricius, 2003; Voss and Richardson, 2006; Haapkylä *et al.*, 2011; Wilson *et al.*, 2012). Such run-off events can also cause harm more indirectly, through eutrophication, hypoxia (Fabricius, 2005; Altieri *et al.*, 2017) and decreased water quality. As global climate change is expected to enhance the frequency and intensity of extreme storm events (Groisman *et al.*, 2005), it is increasingly important to better understand how such storms impact coastal ecosystem functioning.

The western North Pacific, where there is an average of 27 named storms per year (Wang *et al.*, 2010; Herbeck *et al.*, 2011), is the most active region in the world for tropical cyclones. Landfalling typhoons, which most affect coastal ecosystems, have intensified in the region; the proportion of category 4 and 5 typhoons striking land more than doubled in the last four decades. Current climate models predict continued intensification of landfalling typhoons affecting mainland China, Taiwan, Korea and Japan, indicating these regions will suffer even more storm-caused losses of life, property, and coastal habitat (Mei and Xie, 2016). Okinawa Island—the largest island of the Ryukyu archipelago at the edge of the western North Pacific—is an ideal natural laboratory for studying storm effects on coastal ecosystems (Figure 1). Okinawa's coral reefs have experienced significant declines in recent decades, due in part to increased storm induced run-off and sedimentation (Omori, 2011; Hongo and Yamano, 2013; Harii *et al.*, 2014), which is exacerbated by agricultural practices and large coastal development projects (Omija, 2004; Masucci and Reimer, 2019). The fine-particle, laterite soils with high iron concentrations found in Okinawa and typical to the region are easily suspended and turn coastal

86 waters a deep, cloudy red color during the frequent tropical cyclones (Supplemental Figure 1)
87 (Omija, 2004). These events are locally referred to as Red Soil Pollution (Omori, 2011).
88
89 While the biological consequences of storm-induced run-off have been investigated for corals
90 and fish species in Okinawa (Hongo and Yamano, 2013; Inoue *et al.*, 2014; Yamazaki *et al.*,
91 2015; O'Connor *et al.*, 2016; Yamano and Watanabe, 2016), less is known about how tropical
92 cyclones and associated run-off affects coastal microbial communities and especially bacteria
93 (Blanco *et al.*, 2008). Microbial communities contribute to marine ecosystems through primary
94 production and by recycling dissolved organic carbon and nutrients through the microbial loop
95 (Azam *et al.*, 1983), but can also draw down dissolved oxygen (Anderson and Taylor, 2001) or
96 cause opportunistic infections in marine organisms (Shinn *et al.*, 2000; Sutherland *et al.*, 2011;
97 Sheridan *et al.*, 2014; Peters, 2015). Therefore, changes in microbial community compositions
98 in response to storms could precipitate large-scale ecosystem effects. Microbial responses can
99 occur extremely quickly; Gammaproteobacteria, Flavobacteria and many Alphaproteobacteria
100 can increase in abundance within hours when exposed to high nutrient concentrations, whereas
101 the entire microbial community—including archaea, protists, and viruses—can turn over on the
102 scale of less than one day to about a week (Fuhrman *et al.*, 2015). Rapid microbial response
103 times to changing environmental conditions make microbes valuable early-warning bioindicators
104 (Glasl *et al.*, 2017; Pearman *et al.*, 2018), but also hinders their study. Sampling at the scale of
105 microbial response times during tropical cyclones is often dangerous and is further complicated
106 by the poor predictability of storm tracks and intensities (Zhou *et al.*, 2012).
107
108 In this study, we characterize nearshore bacterial community dynamics in response to tropical
109 cyclones affecting Okinawa Island and isolate the effects of sediment input through controlled
110 mesocosm experiments. The study included tropical storm Gaemi at the start of the 2018
111 Okinawa typhoon season (June 16) and successive category 5 super typhoons, Trami and

Kong-Rey, on September 30 and October 5, towards the end of the 2018 season. We evaluated physicochemical properties and bacterial community compositions in seawater samples collected before, during/between, and after storms in June and October and in samples taken from mesocosms with and without red soil amendment. The specific aims for this study were to: i) assess how bacterial community composition and physicochemical parameters respond in time to tropical cyclones and sediment input, ii) evaluate the speed of the responses and recovery, and iii) identify potential ecosystem consequences due to extreme storms and sediment input.

Results

Physicochemical responses to extreme storm events and red soil input

Two major storm events affecting Okinawa Island were monitored for this study. The first event included tropical storm Gaemi, which made landfall on June 16 and was the first tropical cyclone of the 2018 typhoon season. Gaemi brought 133.72 mm day^{-1} of precipitation and maximum wind speeds of 12.1 m s^{-1} to Okinawa (Figure 2). Substantial precipitation and wind were also recorded during the two days leading up to Gaemi's landfall (69.77 and 83.99 mm day^{-1} precipitation and 10.2 and 12.1 m s^{-1} wind intensity on June 14 and 15, respectively), but no additional rain was recorded until July (Figure 2). The second event included two category 5 super-typhoons, Trami and Kong-Rey, which impacted Okinawa in rapid succession towards the end of the 2018 season (Sept. 29 and Oct. 5). Trami and Kong-Rey caused accumulated rainfall of 239.24 and 87.89 mm day^{-1} and maximum wind speeds of 26.9 and 12.7 m s^{-1}, respectively. The June and October events represented the two largest rainfalls during the 2018 typhoon season, and typhoon Trami recorded the most extreme sustained and gusting wind speeds in 2018 (Figure 2). The extreme winds accompanying Trami and Kong-Rey also caused large

waves; Trami and Kong-Rey both brought waves with heights greater than nine meters (Japan Meteorological Agency, https://www.data.jma.go.jp/gmd/kaiyou/shindan/index_wave.html).

Temperature (˚C), salinity (‰) and turbidity (NTU) were measured *in situ* at the four nearshore field sites (A1–4, Figure 1) at the same time that water samples were collected. There was a significant decrease in salinity (~15‰) and concurrent increase of turbidity (~10-fold) during the storm on June 16 compared to before the storm on June 13 and afterwards on June 19 (Figure 3). Up to a 5‰ decrease in salinity and 3 NTU increase in turbidity was measured between the two storms in October (Oct 1 and 3). These changes were smaller in magnitude than were recorded for the June storm and were not statistically significant, despite the storms in October delivering much more precipitation than the June storm (Figure 2). However, the wind accompanying the October storms was also much more intense (Figure 2), which presumably mixed the water column more thoroughly and prevented freshwater lenses from forming, thus contributing to diminished changes in salinity and turbidity being observed in October compared to June.

Concentrations of dissolved nutrients—including Nitrate (NO_3^-), Nitrite (NO_2^-), Ammonium (NH_4^+), Phosphate (PO_4^{3-}), Silica (SiO_2), and dissolved Iron (dFe)—were measured in seawater samples collected in June and October (Figure 3) and throughout the second mesocosm experiment (Supplemental Figure 6). Overall, dissolved nutrient concentrations were higher in June than October, with the exception of dFe and SiO_2, which both had similar values in the two sampling months (Figure 3). A nonparametric Kruskall-Wallis test was applied to detect significant storm-induced differences in field nutrient concentrations (Supplemental Table 3). Results showed significant increases ($p < 0.05$) in NO_2^- concentrations during and following storm events in June and October, whereas SiO_2 and PO_4^{3-} were only significantly elevated during and after the storm in June (Figure 3).

Red soil addition in the October mesocosm experiment caused a significant increase in SiO_2 concentration (Supplemental Figure 6, Supplemental Table 4). Additionally, red soil addition caused PO_4^{3-} concentration to increase above the detection limit 4 hours following soil addition, whereas the concentration of PO_4^{3-} stayed below the detection limit in control mesocosms after the initial measurement (Supplemental Figure 6). Two-way ANOVA results (Supplemental Table 4) indicate that time had a greater effect on nutrient concentration ($p < 0.05$ for NO_2^-, SiO_2 and dFe) than red soil treatment ($p < 0.05$ for SiO_2 and dFe). The treatment by time interaction was only significant in the case of SiO_2 ($p < 0.05$), for which higher concentrations were found in soil-treated mesocosms.

Bacterial community responses to storm events and red soil input

Metabarcoding with the bacterial 16S ribosomal RNA gene was performed to evaluate shifts in bacterial community composition associated with extreme storms in the field and with sediment input in mesocosms. There was a clear shift in the relative abundances of bacterial phyla in field samples collected during the June storm compared to before or afterwards. Several phyla that were also present in soil samples became more abundant in the water samples collected during the storm—including Acidobacteria, Actinobacteria, Chloroflexi, Firmicutes, Rokubacteria and Verrumicrobia—but phyla not detected in soil samples also became more abundant during the storm, most notably Epsilonbacteraeota (Figure 4). Principal component analysis (PCA) of Aitchison distances between bacterial community compositions in water samples also clearly illustrated a shift in community composition during the June storm; samples collected during the storm separated along the primary axis (PC1) from the samples collected both before and afterwards (Figure 5). The shift in community composition during the storm was accompanied by an increase in ASV richness (Amplicon Sequence Variants; Figure

6); estimated ASV richness was significantly higher in samples collected during the June storm compared to samples collected before and afterwards.

Soil addition to June mesocosms also influenced bacterial community composition and richness, although to a lesser extent than the storm-influenced nearshore communities. Bacterial phyla dominant in soil samples were detectable in mesocosm samples taken one hour after soil addition, but their relative abundance diminished in samples taken 24 hours later (Figure 4). Likewise, ASV richness increased in samples taken from mesocosms following soil addition and decreased over time (Supplemental Figure 8). Overall, mesocosm incubation time had a larger effect on bacterial community composition than soil addition (Figure 4, Supplemental Figure 9), despite mesocosm conditions (temperature, salinity, dissolved oxygen) remaining similar to ambient conditions throughout the experiment (Supplemental Figures 4–5).

In October, the community composition also shifted between the two storms (Trami and Kong-Rey) relative to before and after the overall event window. Additionally, some phyla present in soil samples, particularly Firmicutes, increased in relative abundance within the event window, but similar to in June, phyla undetected in soil samples also increased in relative abundance (e.g. Epsilonbacteraeota and Fusobacteria). However, unlike in June, Actinobacteria, Planctomycetes, and Verrucomicrobia were already detectable in water samples collected before Typhoon Trami affected Okinawa (Figure 4). PCA further demonstrated a shift in community composition in samples collected between the October storms compared to before and afterward; samples collected between the two storms separated on the primary axis from samples collected before and after the storms (Figure 5). Interestingly, the estimated ASV richness was lower (by about half) for all samples collected in October compared to in June, including in soil samples, and estimated richness did not increase in the samples collected between storms (Figure 6). Community compositions in field samples from the different months segregated along the primary axis in PCA and the differences were statistically significant using PERMANOVA ($p < 0.01$, $F = 5.37$, $R^2 = 0.17$), demonstrating that nearshore bacterial

communities were distinct in June and October (Supplemental Figure 7). Furthermore, soil addition to October mesocosms did not cause observable increases in relative abundances of phyla found in soil samples as it had in June (Figure 4, Supplemental Figure 8).

In order to identify individual taxa that became more abundant during storms and, thus, contributed to the broader patterns observed in the data, we performed pairwise testing for differentially abundant ASVs between sampling dates in each month. The greatest number of significantly differentially abundant ASVs were found in the pairwise test between June 13 (before the storm) and June 16 (during the storm), with the vast majority being more abundant during the storm (Figure 7A). In contrast, very few ASVs were significantly differentially abundant in samples collected before and after the June storm (Figure 7A). While many of the ASVs that had significantly higher relative abundance during the storm on June 16 were also detected in soil samples, the majority were not (Figure 7A, B). ASVs that had significantly higher relative abundance on June 16 compared to June 13 belonged to a total of 67 orders—including Flavobacteriales, Campylobacterales, and Vibrionales, which can be pathogenic to humans and marine organisms (Pruzzo *et al.*, 2005; Silva *et al.*, 2011; Loch and Faisal, 2015; Canty *et al.*, 2020), and Rhizobiales, Sphingomonadales, and Alteromonadales, which were also found in soil samples (Figure 7B). In pairwise tests for October samples, the largest number of differentially abundant ASVs were likewise found between samples collected before (Sept. 28) and between storms (Oct. 1 and 3), but none of the differentially abundant ASVs were also found in soil samples (Figure 7C, D). ASVs showing significant differences in relative abundance between samples taken before and between the October storms belonged to 21 different orders, with most, but not all, also represented in the June results (Figure 7D).

Discussion

As the severity and frequency of extreme storm events increases with global climate change, it is increasingly important to understand how these events impact ecological functioning in marine ecosystems (Wetz and Paerl, 2008; Du *et al.*, 2019). However, characterizing the effects of extreme storm events, such as typhoons, on coastal ecosystems is a complicated task, due both to forecast unpredictability, which makes sampling before and after events challenging, and the dangerous conditions that accompany storms (Chen *et al.*, 2018). This study reports on the nearshore microbial community dynamics and relevant environmental parameters during two short sampling campaigns encompassing major storms of the 2018 typhoon season in Okinawa, Japan. In addition, concurrent, controlled mesocosm experiments were performed to supplement field observations and isolate impacts of terrestrial sediment input that regularly accompanies large storms in Okinawa. Predictably, storms caused influxes of both freshwater and sediment into the coastal marine environment (Figure 3, Supplemental Figure 1), which carried some soil-derived bacteria and some bacteria presumably derived from other terrestrial sources (e.g. urban or agricultural wastewater; Figures 4 and 7). The storm effects were short-lived, however, and bacterial community compositions in samples collected before and after storms were largely similar (Figures 4, 5, 7). While field samples were collected three days after storm events, mesocosm experiments showed that bacteria introduced with soil additions diminished in relative abundance just four hours after soil input and were no longer detectable 24 hours later. Despite the rapidity of community shifts, terrestrially derived bacteria and marine bacteria that increased in relative abundance during and after storms may still influence coastal biogeochemical cycling and, in some cases, could be detrimental to the coastal ecosystem or dangerous to human health. For instance, Rhodobacteraceae bacteria (order Rhodobacterales), which became relatively more abundant during storms (Figure 7), are known to rapidly and competitively exploit transient sources of particulate and dissolved organic matter and thus may enhance remineralization in nearshore waters (Buchan *et al.*, 2014). Other bacteria that increased in relative abundance during and after storms can cause diseases in reef-building

corals (e.g. *Vibrio spp.*, *Pseudoalteromonas sp.*) and humans (e.g. Campylobacter, Fusobacteria, Enterobacter) (Pruzzo *et al.*, 2005; Vizcaino *et al.*, 2010; Silva *et al.*, 2011; Zimmer *et al.*, 2014); Figure 7, Supplemental Tables 6 and 7), emphasizing the need to better understand sources and sinks of these bacteria in the coastal environment.

Extreme storms cause rapid changes in environmental conditions and bacterial community composition

During the storm event in June, we measured decreased salinity and increased turbidity in nearshore surface waters (Figure 3), which is similar to previous reports following major storm events (De Carlo *et al.*, 2007; Zhou *et al.*, 2012; Chen *et al.*, 2018). Freshwater and sediment input was accompanied by moderate increases in NO_2^-, NO_3^-, NH_4^+, PO_4^{3-}, SiO_2 and dFe concentrations that ranged from a few nM, in the case of dFe, to up to 25 µM for SiO_2 (Figure 3) and is consistent with terrestrial run-off from agricultural areas with high iron-content soil, as is found in Okinawa (Arakaki *et al.*, 2005). However, nutrient loading dissipated before samples were collected again three days after the June storm (Figure 3). Bacterial diversity (ASV richness, Figure 6) increased during the storm, representing the introduction of bacterial taxa that were also found in our soil samples and are common components of soil microbiomes, including Acidobacteria, Actinobacteria, Chloroflexi, Firmicutes, Planctomycetes, Rokubacteria and Verrucomicrobia (Figure 4; Freitas *et al.*, 2012; Witt *et al.*, 2012; Balmonte *et al.*, 2016; Lin *et al.*, 2019). Many of these taxa are also commonly associated with particulate matter in marine environments (e.g. Planctomycetes, Actinobacteria, and Verrucomicrobia) making resuspension of marine sediment during storms another potential contributing source of these bacteria (DeLong *et al.*, 1993; Crespo *et al.*, 2013). Campylobacterales (Epsilonbacteraeota) that increased in relative abundance during storms could also derive from agricultural waste being incorporated into run-off (Jones, 2001).

Three days after the storm, on June 19, the bacterial diversity returned to pre-storm levels (Figure 6A) and the community composition was almost identical to before the storm (Figure 5A). Moreover, only 19 ASVs were significantly differentially abundant between June 13 and June 19 compared to 267 ASVs between June 13 and June 16 (Figure 7A), demonstrating the high speed at which the microbial community recovered. This high speed largely contrasts with previous field studies where longer periods of time (i.e. from weeks to months) were needed to restore pre-storm microbial compositions (De Carlo *et al.*, 2007; Yeo *et al.*, 2013). The ephemerality of terrestrially-derived bacteria after introduction to the coastal environment was similarly apparent in results from the June mesocosm experiment. We detected phyla dominant in soil samples (e.g. Acidobacteria, Chloroflexi, Firmicutes, and Planctomycetes) in treatment mesocosms one hour after soil was added, but the relative abundances of these phyla decreased in samples taken four and twelve hours later, and they were no longer detectable in samples taken 24 hours later. The transience of storm-effects on nearshore bacterial communities was further demonstrated in results from the October storm event. The bacterial community recovered just three days after super-typhoon Kong-Rey passed, the second super-typhoon to affect Okinawa in less than a week (Figure 5B). This transience may, in part, reflect terrestrial and freshwater bacteria lysing in seawater due to osmotic stress. However, enteric bacteria are able to survive in seawater, particularly when organic material is readily available (Munro *et al.*, 1989). Settling was likely also a contributing factor, as many of the bacterial taxa that increased in relative abundance during storms and after soil addition to mesocosms are known to associate with sediment surfaces (DeLong *et al.*, 1993; Duret *et al.*, 2019) and some sedimentation was visible in mesocosm bottles despite using pumps to maintain water circulation. Moreover, tidal flushing may have transported introduced or resuspended bacteria offshore.

Extreme storms cause context-dependent changes in environmental conditions and bacterial community composition

While storm effects were transient in both cases (Figure 5), the June and October storm events affected coastal physicochemistry and bacterial community composition differently (Figures 3, 4). Events in both June and October increased coastal nitrogen loading, but only the June event was accompanied by increased PO_4^{3-} and SiO_2 concentrations, and the June storm caused more pronounced shifts in bacterial community composition, highlighted by a larger increase in ASV richness and a higher number of differentially abundant ASVs (Figure 7). Although these differences in both nutrient loading and bacterial communities, may reflect disparate sampling schemes, it is likely that differences in rain and wind intensity, as well as the contexts in which the two events occurred, had strong effects. It has been shown that wind speed alone can drive alpha diversity shifts in epipelagic bacterial communities (Bryant *et al.*, 2016). Key differences between the June and October events were that much more rain, wind and wave action accompanied the October storm event than the June storm and that the June storm made landfall at the beginning of the typhoon season, whereas the October storms affected Okinawa towards the end of the typhoon season.

Typhoon Trami, on Sept. 29, caused twice as much precipitation as tropical storm Gaemi, on June 16 (Figure 2), which could have diluted nutrient loading in storm run-off and caused the smaller changes in nutrient concentrations recorded in October compared to in June (Figure 3). When flushing rate is high, less PO_4^{3-} is desorbed from sediments and there is a dilution effect for both dissolved phosphorus and nitrogen in run-off (Blanco *et al.*, 2010). Additionally, Gaemi was the first major storm of the 2018 typhoon season (June–October) following a relatively prolonged dry period, which could increase nutrient loading in storm run-off, especially since agricultural fertilizers are applied throughout the preceding spring and summer growing season. By October, several tropical storms and typhoons had already

affected Okinawa (Figure 2); the 2018 Pacific typhoon season had higher than average storm frequency and included 29 tropical storms, 13 typhoons, and 7 super typhoons, although not all made direct landfall with Okinawa (Japan Meteorological Agency, https://www.jma.go.jp/jma/indexe.html). These intervening events could strip topsoil and deplete soil nutrients and microbiomes, so that October storm run-off carried less nutrients, organic material, and terrestrial bacteria into coastal water than storm run-off in June. Moreover, antecedent soil moisture affects dissolved nutrient loading in run-off, with less nutrients desorbing from clay-based soils, like Okinawa red soil, when already wet (Perrone and Madramootoo, 1998).

The controlled mesocosm experiments offer additional insight for interpreting differences in field observations between June and October. Despite collecting soil from the same place in June and October, the soil microbiome in October had half the bacterial richness as in June (Figure 6) and soil addition to October mesocosms did not introduce soil bacteria or increase bacterial richness as it had in June mesocosms (Figure 4, Supplemental Figure 9). These results suggest that run-off from storms occurring towards the end of the typhoon season may carry less diverse bacterial assemblages than run-off from early-season storms. Furthermore, soil addition in October mesocosms did not cause nitrogen (NO_2^- or NO_3^-) or dFe to increase over baseline measurements, but did cause increases in SiO_2 and PO_4^{3-} (Supplemental Figure 6). However, the increase in SiO_2 and PO_4^{3-} were gradual, demonstrating that time is required to release these compounds from red soil (De Carlo *et al.*, 2007; Blanco *et al.*, 2010; Chen *et al.*, 2018). Soils in Okinawa could, therefore, have lower nitrogen content at the end of the typhoon season and more intense rains may deliver less nutrients due to rapid flushing.

Influence of extreme storms on bacterial taxa in nearshore waters

The influence of June and October storms on coastal microbial communities varied in effect size, but in both instances the community shift was rapid and transient and included shared bacterial groups that became more abundant during and after storms in both months; 15 out of the 21 bacterial orders encompassing ASVs that were significantly more abundant during the October event were shared with the June event (Figure 7). The shared bacterial orders included primarily heterotrophic bacteria, several of which contain potentially pathogenic groups (e.g. Vibrionales, Fusobacteriales, and Campylobacterales) (Pruzzo et al. 2005; Silva et al. 2011; Canty et al. 2020). Originally, we expected cyanobacteria to respond to increased inorganic nutrients delivered to the coastal ecosystem with storm run-off. Specifically, we expected nitrogen fixers—such as *Trichodesmium*, which occasionally blooms near Okinawa (Grossmann *et al.*, 2015)—to benefit from increased dFe and PO_4^{3-} in run-off (Sañudo-Wilhelmy *et al.*, 2001; Wu *et al.*, 2003). Instead, only a few cyanobacteria ASVs became more abundant during the June storm, but not the October storm (Figure 7). Namely, cyanobacteria belonging to the family Oscillatoriaceae, which form filamentous benthic mats (Siegesmund *et al.*, 2008; Engene *et al.*, 2018), and Obscuribacterales, which are uncultured and have unknown morphology, but may not be photosynthetic (Soo *et al.*, 2014), became more abundant in June.

There are several possible explanations for the minimal changes in cyanobacteria relative abundance: i) cyanobacteria were not limited by compounds present in run-off, ii) nutrients in run-off were not biologically available, or iii) terrestrial run-off was transported offshore or diluted too quickly to affect nearshore communities. Nutrient concentrations that were elevated during the June storm (NO_2^-, NO_3^-, PO_4^{3-} and dFe) decreased after the storm passed, but not immediately and not as quickly as microbial communities recovered (Figures 3, 4). Since these nutrients were not immediately drawn down, the photosynthetic microbial community may not have been nutrient limited in our study area. That microbial communities did not respond to soil addition in mesocosms, despite increased PO_4^{3-} and dFe, further suggests that nutrient availability was not driving major changes in bacterial community composition.

Heterotrophic bacteria increasing in relative abundance during and after storms could derive from soil or other components of run-off, have been resuspended from the seafloor due to wind and waves, or have responded to increased organic matter from run-off. These bacteria may affect ecosystem functioning by remineralizing organic matter within the near-shore environment (Buchan et al. 2014; Kieft et al. 2018) or by causing opportunistic infections in keystone metazoans (Pruzzo et al. 2005; Silva et al. 2011; Canty et al. 2020), thus making it important to identify their source. Rare bacteria often become more abundant during or after disturbances (Preisner et al. 2016; Fuentes et al. 2016; Sjöstedt et al. 2012), but it is difficult to parse out their sources (Shade et al. 2014). Such conditionally rare bacteria may result from introductions or opportunistic growth of previously undetectable bacteria (Shade et al. 2014). Discriminating between these potential sources is challenging with current methods, but prolonged intensive sampling better resolves the dynamics of rare taxa (Shade et al. 2013; Shade et al. 2014). Beyond working towards establishing the more long term dynamics of nearshore bacterioplankton communities, future work aimed at characterizing bacteria in wastewater outflows and stormwater could also help determine whether bacteria that become more abundant during storms represent introductions or expansions.

Potential ecosystem consequences due to terrestrial run-off from extreme storms

Despite being short-lived, the changes we observed in bacterial community composition and environmental parameters during storms can nevertheless be detrimental to both the coastal ecosystem and human health. While most terrestrially-derived bacteria are benign to marine ecosystems, many are potentially pathogenic to corals and other marine organisms (Sutherland *et al.*, 2004; Haapkylä *et al.*, 2011; Pollock *et al.*, 2014; Sheridan *et al.*, 2014). Terrestrial run-off has been implicated in coral diseases, such as White Pox Disease and Red Band Disease, in many tropical and subtropical locations, including Madagascar (Haapkylä *et al.*, 2011; Pollock *et*

418 *al.*, 2014; Sheridan *et al.*, 2014), the Caribbean (Frias-Lopez *et al.*, 2002; Patterson *et al.*,
419 2002), and Australia's Great Barrier Reef (Pollock *et al.*, 2014). Furthermore, storm events can
420 cause water-column mixing and sediment resuspension, leading to pathogenic marine bacteria
421 that usually inhabit the seafloor to become more abundant in the water column (Hassard *et al.*,
422 2016). Indeed, in our study we found several strains of *Vibrio spp.*, *Pseudoalteromonas sp.*, and
423 Rhodobacteraceae bacteria specifically associated with coral disease (Sussman *et al.*, 2008;
424 Sheridan *et al.*, 2014) to be significantly enriched in samples we collected during or following
425 storm events (Supplemental Table 5). Considering the additional stress caused by turbidity and
426 sedimentation during storm events, alongside potentially decreased pH and dissolved oxygen
427 due to enhanced heterotrophic bacterial respiration (Weber *et al.*, 2012; Altieri *et al.*, 2017),
428 corals and other organisms may be especially susceptible to pathogen infection during and after
429 extreme storms.
430
431 Heavy rains and floods have long been implicated in transporting human pathogens (e.g. fecal
432 coliform bacteria) to the marine environment (Pandey *et al.*, 2014; De Jesus Crespo *et al.*,
433 2019). Indeed, we found bacterial taxa that are potentially dangerous to humans—including
434 Campylobacterales, Fusobacteriales, Bacillales, Clostridiales and Enterobacteriales (Bennett
435 and Eley, 1993; Sharma *et al.*, 2003; Davin-Regli *et al.*, 2019)—significantly enriched during and
436 following storms. Many of these bacteria were not detected in soil samples, suggesting
437 additional sources of bacterial contamination in storm run-off. For instance, some of the
438 Bacillales and Enterobacterales ASVs enriched in storm-influenced water samples were not
439 present in soil samples and none of the enriched Clostridiales, Campylobacterales and
440 Fusobacteriales ASVs were also found in soil samples (Figure 7). Likewise, these taxa were not
441 found in mesocosms following soil addition in June or October, demonstrating the larger effect
442 of storms and run-off on the coastal ecosystem than simply transporting sediment into the
443 water. Human pathogens may derive from live-stock, storm drains, or overwhelmed waste

444 treatment plants during storms (Weiskel *et al.*, 1996; Jamieson *et al.*, 2004). Interestingly, these
445 taxa were already present in water samples collected on September 28—although they were
446 more abundant on October 1 and 3—further indicating a cumulative effect of the typhoon
447 season on the coastal ecosystem and emphasizing the context-dependency of storm effects.
448 Ultimately, swimmers and other recreational users need to be aware that pathogenic bacteria
449 are likely present in Okinawa coastal waters following large rain events. This is not currently the
450 case in Okinawa as it is in other locations with more robust coastal monitoring programs in
451 place (e.g. the Southern California Water Research Project or the DNAqua-Net European
452 project).
453
454 **Conclusions & Future Directions**
455
456 Despite challenges associated with sampling marine ecosystems during tropical storms and
457 typhoons, this study describes the timing and nature of storm effects on coastal bacterial
458 communities in Okinawa, Japan. We found that storm effects were transient, but highly context-
459 dependent. We coupled controlled mesocosm studies with field observations in an effort to
460 disentangle the effects of extreme wind and waves and enhanced currents from the effects of
461 soil input during storms. While the mesocosm results were useful, future studies would benefit
462 from more realistic run-off simulation (e.g. Le *et al.*, 2016) than the soil additions we employed.
463 Furthermore, it remains that we did not perform bacterial cell counts or otherwise measure
464 bacterial biomass or metabolic activity, thus leaving the possibility that run-off increased
465 microbial biomass or differentially affected microbial physiology. Future studies may capture
466 such responses by measuring bacterial respiration rates or by performing metatranscriptomics.
467
468 It is important to note that environmental effects of extreme storms will vary in terms of intensity,
469 spatial extent and duration in different ecosystems and need to be evaluated locally (Paerl *et al.*,

2006; Zhang *et al.*, 2009; Herbeck *et al.*, 2011). Storm effects were transient in the open, tidally-flushed Okinawa coast, but more prolonged storm effects have been observed in other coastal systems, particularly semi-enclosed areas, such as bays and estuaries, where terrestrial sediment loads can have residence times from weeks to years (Paerl *et al.*, 2001; Zhang *et al.*, 2009; Herbeck *et al.*, 2011). Therefore, we suggest that the short-term study of typhoon events follow an adaptive sampling strategy (Wetz and Paerl, 2008), which involves the definition of well-established baselines for various physicochemical and biological parameters.

Finally, the transient nature of storm effects described here should not be viewed as diminishing their potential impact on reef or human health. Differentially abundant bacteria during storms may cause disease in marine organisms and humans. With future climate change scenarios predicting more frequent and destructive storms and continued expansion of tourism and agriculture activities, it is likely that the amount of terrestrial run-off and associated risks will escalate in the future. This makes regional monitoring programs, including a comprehensive understanding of background conditions, essential for better interpretations of ecological consequences from extreme storm events.

Experimental Procedures

Study setting

Seawater was collected for metabarcoding and physicochemical analysis from four nearshore sampling points approximately 250–500 m apart, along the central west coast of Okinawa Island—a semi-urban region with mixed land-use, including agriculture and coastal development projects (Figure 1). The sampling points (A1–4) were each at least 1.2 km from the nearest concentrated fresh-water input (e.g. streams or rivers). At the start of the 2018 typhoon season,

samples were collected before (June 13), during (June 16), and after (June 19) tropical storm Gaemi, which struck Okinawa on June 16, 2018 and caused a red soil pollution event (Figure 2, Supplemental Figure 2A). Towards the end of the typhoon season, samples were collected before (Sept 28), during (Oct 1 and Oct 3) and after (Oct 8) a red soil pollution event caused by typhoon Trami, which made landfall with Okinawa on September 30, and was prolonged by Typhoon Kong-Rey, which approached Okinawa on October 5th (Figure 2, Supplemental Figure 2B–C).

Seawater sampling for DNA and physicochemical analysis

Surface seawater was collected for DNA metabarcoding by submerging clean 500 mL Nalgene bottles just below the sea surface. Seawater for dissolved Fe (dFe) and nutrient analysis was collected in acid-cleaned 50 mL Falcon tubes. Physicochemical properties—dissolved oxygen (DO), salinity, temperature, and turbidity—were measured with a CTD probe (RINKO, JFE Advantech, Japan) at each site. After being immediately transported to the laboratory, seawater samples for metabarcoding were filtered through 0.2 µm pore-size Polytetrafluoroethylene (PTFE) filters (Millipore) under gentle vacuum and filters were stored at -20 ˚C for later DNA extraction. Seawater samples for dFe and nutrient analysis were filtered through 0.45 µm pore-size acid-washed Teflon digiFILTERS (SPC Science, Canada) and filtered water samples were stored at -20 ˚C for later chemical analysis.

Mesocosm experimental design

Seawater was collected for concurrent mesocosm experiments on June 11 (26.512 ˚N, 127.872˚E) and October 10 (26.479 ˚N, 127.829 ˚E). Nearshore coastal seawater was pumped from just below the sea surface and filtered through 1 mm and 300 µm nylon mesh screen sizes to remove debris and larger organisms. Acid-cleaned 22 L clear-plastic carboys were rinsed twice with 300 µm nylon mesh-size filtered seawater before filling to 20 L with filtered seawater.

Bottles were covered with parafilm and kept shaded during transport to the Okinawa Institute of Science and Technology (OIST) Marine Science Station, where they were submerged in a basin with continuous flow-through seawater to keep conditions within the bottles similar to natural conditions. Mesocosm bottles were topped with silicone sponge stoppers to allow gas exchange, but limit evaporation and prevent dust, water or other contaminants from entering the bottles during the experiment (Supplemental Figure 3). Small pumps were included in each mesocosm to maintain water circulation (2 L min^{-1}). HOBO temperature and light loggers (Onset) were fastened to the pumps and at the same depth in the basin surrounding mesocosms to ensure that mesocosms conditions remained similar to ambient conditions (Supplemental Figure 4). Salinity and DO were measured each time water was sampled from the mesocosms throughout the experiment (Supplemental Figure 5). Mesocosms experiments included 9–10 mesocosms: 4–5 control replicates (four in June and five in October) and 5 treatments replicates with red soil added to an ecologically relevant high concentration of 200 mg L^{-1} (O'Connor *et al.*, 2016). Mesocosms were sampled (100 mL for metabarcoding, 50 mL for dFe and nutrient concentration) with 50 mL sterile pipettes before the experiment started (t0), and 1, 4, 12, 24, and 48 h following red soil addition to treatment bottles. Water samples were processed as described in the previous section.

Red soil collection for mesocosm experiments and DNA analysis

Soil samples were collected from an open agricultural field with exposed soil (26.507 ˚N, 127.868 ˚E), on June 10 and October 9 for addition to red soil treated mesocosms and to evaluate soil microbiomes. Soil samples were sieved through 330 µm mesh and maintained at 4 °C for 24 h until use in the mesocosm experiment. To determine soil moisture content, 10 g subsamples (n=10) were weighed and dried at 100 °C by following the standard method AS 1289.2.1.1-2005 (Standards Association of Australia). Soil moisture content was used to calculate how much wet soil should be added to mesocosms in order to reach the final

concentration of 200 g soil (dry weight) per L seawater. In both June (n=4) and October (n=2), additional 50 g aliquots of soil were kept at -20 °C for subsequent metabarcoding analysis.

Chemical analysis: dFe and major nutrients

Dissolved Fe (dFe) concentration was determined following the methodology of Wu and Boyle (1998). This method uses a Mg $(OH)_2$ co-precipitation to pre-concentrate Fe from seawater followed by an isotope dilution method. Seawater dFe was quantified using an internal standard element (^{57}Fe) with inductively coupled plasma mass spectrometry (Element 2, Thermo Scientific). The mass spectrometer was operated in medium-resolution mode with 4000 resolution (FWHM). The mass calibration was performed using a multi-element ICP-MS tune-up solution (Thermo Fisher Scientific). In order to ensure the quality of the ICP-MS analysis, control standards and samples (i.e. analytical replicates, certified reference material and analytical blank) were analyzed once every 12 samples. Recovery of Fe from reference certified material QC3163 (Sigma-Aldrich, USA) was satisfactory and ranged from 65 to 80%. The overall error associated with the analytical process was typically lower than 5% and never higher than 15%. All measurements were above the instrument's detection limit. Analysis was carried out at the OIST Instrumental Analysis Section mass spectrometry laboratory. Special attention was paid to avoid Fe contamination and an exhaustive cleaning process was carried out following the methods of(King and Barbeau, 2011).

Nutrient concentrations—including Nitrate (NO_3^-), Nitrite (NO_2^-), Ammonium (NH_4^+), Phosphate (PO_4^{3-}) and Silica (SiO_2)—were determined on a QuAAtro39 Continuous Segmented Flow Analyzer (SEAL Analytical) following manufacturer guidelines. Final concentrations were calculated through AACE software (SEAL Analytical). Nutrient Analysis was carried out at the Okinawa Prefecture Fisheries and Ocean Technology Center.

Nutrient and dFe statistical analyses

Mesocosm data were found to be normally distributed with a Shapiro-Wilks test and, therefore, a one-way ANOVA was performed to test overall differences between treatments. Post-hoc Tukey HSD analysis was performed to identify which specific groups differed. Field data were not normally distributed, regardless of transformation, so a Kruskal-Wallis test was used to test for significant differences between sampling dates. Analyses were performed within the R statistical environment (R Core Team 2018).

DNA extraction and metabarcode sequencing

DNA was extracted from frozen PTFE filters following the manufacturer protocol for the DNeasy PowerWater Kit (Qiagen), including the optional heating step. DNA was extracted from soil samples by following manufacturer protocol for the DNeasy PowerSoil Kit (Qiagen). Metabarcode sequencing libraries were prepared for the V3/V4 region of the bacterial 16S ribosomal RNA gene following Illumina's "16S Metagenomic Sequencing Library Preparation" manual without any modifications. Sequencing libraries were transferred to the OIST Sequencing Center for 2x300-bp sequencing on the Illumina MiSeq platform with v3 chemistry. Overall, 18.4 million sequencing reads were generated in this study, with 76,217–219,584 sequencing reads per sample (mean = 137,585). Sequencing data are available from the NCBI Sequencing Read Archive under the accession PRJNA564579.

Metabarcode analyses

Sequencing reads were denoised using the Divisive Amplicon Denoising Algorithm (Callahan *et al.*, 2016) with the DADA2 plug-in for QIIME 2 (Bolyen *et al.*, 2019). Following denoising, 11.8 million sequences remained with 11,061–153,646 sequences per sample (mean = 88,033). A total of 36,007 ASVs were identified in our dataset, with 64–2,886 unique ASVs observed per

sample (mean = 642). Taxonomy was assigned to representative ASVs using a Naive Bayes classifier trained on the SILVA 97% consensus taxonomy (version 132, Quast *et al.*, 2013) with the QIIME 2 feature-classifier plug-in (Bokulich *et al.*, 2018). The results were imported into the R statistical environment (R Core Team 2018) for further analysis with the Bioconductor phyloseq package (McMurdie and Holmes, 2013). The ASV richness for each sample was estimated using the R package breakaway (Willis and Bunge, 2015) and differences in estimated richness between sample types were tested for with the betta function (Willis *et al.*, 2017). In order to minimize compositional bias inherent in metabarcoding data as much as possible, we used the Aitchison distance between samples, which includes a centered log ratio transformation to normalize data (Gloor *et al.*, 2017), for principal component analyses (PCA). Permutational analyses of variance (PERMANOVA) on Aitchison distances were performed with the adonis function (999 permutations) in the R package vegan (Oksanen *et al.*, 2019) to test whether shifts in community composition were statistically significant. Lastly, we used the DESeq2 bioconductor package (Love *et al.*, 2014) to determine which ASVs were significantly differentially abundant (False Discovery Rate adjusted p-value < 0.05) in water samples collected from field sites before, during, and after storms. We then checked if significantly differentially abundant ASVs were also present in soil samples from respective months to assess whether differentially abundant ASVs were soil-derived. Intermediate data files and the code necessary to replicate analyses are available in a GitHub repository: https://github.com/maggimars/RedSoil.

Acknowledgments

We thank Akinori Murata and Marine Le Gal for help with sample collection, Kazumi Inoha, Koichi Toda, Kosuke Mori and Okinawa Marine Science Support Section, OIST for assistance with experimental design and technical support and Koichi Kinjo from the Okinawa Prefectural

Institute of Health and Environment for his advice. We also thank OIST sequencing center for DNA sequence support and Okinawa Prefecture Fisheries and Ocean Technology Center for nutrient analysis assistance. MMB was supported by a Japan Society for the Promotion of Science (JSPS) DC1 graduate student fellowship. This work was supported by the JSPS KAKENHI program [Early-Career Project No. 18K18203] and the OIST Marine Biophysics Unit. Furthermore, we confirm that we have no conflicts of interest to disclose.

Reference list

Altieri, A.H., Harrison, S.B., Seemann, J., Collin, R., Diaz, R.J., and Knowlton, N. (2017) Tropical dead zones and mass mortalities on coral reefs. *Proc Natl Acad Sci U S A* **114**: 3660–3665.

Anderson, T.H. and Taylor, G.T. (2001) Nutrient pulses, plankton blooms, and seasonal hypoxia in western Long Island Sound. *Estuaries* **24**: 228–243.

Arakaki, T., Fujimura, H., Hamdun, A.M., Okada, K., Kondo, H., Oomori, T., et al. (2005) Simultaneous Measurement of Hydrogen Peroxide and Fe Species (Fe(II) and Fe(tot)) in Okinawa Island Seawater: Impacts of Red Soil Pollution. *J Oceanogr* **61**: 561–568.

Azam, F., Fenchel, T., Field, J.G., Gray, J.S., Meyer-Reil, L.A., and Thingstad, F. (1983) The Ecological Role of Water-Column Microbes in the Sea. *Marine Ecology Progress Series* **10**: 257–263.

Balmonte, J.P., Arnosti, C., Underwood, S., McKee, B.A., and Teske, A. (2016) Riverine Bacterial Communities Reveal Environmental Disturbance Signatures within the Betaproteobacteria and Verrucomicrobia. *Front Microbiol* **7**: 1441.

Bennett, K.W. and Eley, A. (1993) Fusobacteria: new taxonomy and related diseases. *J Med Microbiol* **39**: 246–254.

Blanco, A.C., Nadaoka, K., and Yamamoto, T. (2008) Planktonic and benthic microalgal community composition as indicators of terrestrial influence on a fringing reef in Ishigaki Island, Southwest Japan. *Mar Environ Res* **66**: 520–535.

Blanco, A.C., Nadaoka, K., Yamamoto, T., and Kinjo, K. (2010) Dynamic evolution of nutrient discharge under stormflow and baseflow conditions in a coastal agricultural watershed in Ishigaki Island, Okinawa, Japan. *Hydrol Process* **24**: 2601–2616.

Bokulich, N.A., Kaehler, B.D., Rideout, J.R., Dillon, M., Bolyen, E., Knight, R., et al. (2018) Optimizing taxonomic classification of marker-gene amplicon sequences with QIIME 2's q2-feature-classifier plugin. *Microbiome* **6**: 90.

Bolyen, E., Rideout, J.R., Dillon, M.R., Bokulich, N.A., Abnet, C.C., Al-Ghalith, G.A., et al. (2019) Reproducible, interactive, scalable and extensible microbiome data science using QIIME 2. *Nat Biotechnol* **37**: 852–857.

Brodie, J.E., Kroon, F.J., Schaffelke, B., Wolanski, E.C., Lewis, S.E., Devlin, M.J., et al. (2012) Terrestrial pollutant runoff to the Great Barrier Reef: An update of issues, priorities and management responses. *Mar Pollut Bull* **65**: 81–100.

Bryant, J.A., Aylward, F.O., Eppley, J.M., Karl, D.M., Church, M.J., and DeLong, E.F. (2016) Wind and sunlight shape microbial diversity in surface waters of the North Pacific

Subtropical Gyre. *ISME J* **10**: 1308–1322.
Buchan, A., LeCleir, G.R., Gulvik, C.A., and González, J.M. (2014) Master recyclers: features and functions of bacteria associated with phytoplankton blooms. *Nat Rev Microbiol* **12**: 686–698.
Callahan, B.J., McMurdie, P.J., Rosen, M.J., Han, A.W., Johnson, A.J.A., and Holmes, S.P. (2016) DADA2: High-resolution sample inference from Illumina amplicon data. *Nat Methods* **13**: 581–583.
Canty, R., Blackwood, D., Noble, R., and Froelich, B. (2020) A comparison between farmed oysters using floating cages and oysters grown on-bottom reveals more potentially human pathogenic Vibrio in the on-bottom oysters. *Environ Microbiol*.
Chen, N., Krom, M.D., Wu, Y., Yu, D., and Hong, H. (2018) Storm induced estuarine turbidity maxima and controls on nutrient fluxes across river-estuary-coast continuum. *Sci Total Environ* **628-629**: 1108–1120.
Chen, N., Wu, J., and Hong, H. (2012) Effect of storm events on riverine nitrogen dynamics in a subtropical watershed, southeastern China. *Sci Total Environ* **431**: 357–365.
Crespo, B.G., Pommier, T., Fernández-Gómez, B., and Pedrós-Alió, C. (2013) Taxonomic composition of the particle-attached and free-living bacterial assemblages in the Northwest Mediterranean Sea analyzed by pyrosequencing of the 16S rRNA. *Microbiologyopen* **2**: 541–552.
Davin-Regli, A., Lavigne, J.-P., and Pagès, J.-M. (2019) Enterobacter spp.: Update on Taxonomy, Clinical Aspects, and Emerging Antimicrobial Resistance. *Clin Microbiol Rev* **32.**:
De Carlo, E.H., Hoover, D.J., Young, C.W., Hoover, R.S., and Mackenzie, F.T. (2007) Impact of storm runoff from tropical watersheds on coastal water quality and productivity. *Appl Geochem* **22**: 1777–1797.
De Jesus Crespo, R., Wu, J., Myer, M., Yee, S., and Fulford, R. (2019) Flood protection ecosystem services in the coast of Puerto Rico: Associations between extreme weather, flood hazard mitigation and gastrointestinal illness. *Sci Total Environ* **676**: 343–355.
DeLong, E.F., Franks, D.G., and Alldredge, A.L. (1993) Phylogenetic diversity of aggregate-attached vs. free-living marine bacterial assemblages. *Limnol Oceanogr* **38**: 924–934.
Du, J., Park, K., Dellapenna, T.M., and Clay, J.M. (2019) Dramatic hydrodynamic and sedimentary responses in Galveston Bay and adjacent inner shelf to Hurricane Harvey. *Sci Total Environ* **653**: 554–564.
Duret, M.T., Lampitt, R.S., and Lam, P. (2019) Prokaryotic niche partitioning between suspended and sinking marine particles. *Environ Microbiol Rep* **11**: 386–400.
Engene, N., Tronholm, A., and Paul, V.J. (2018) Uncovering cryptic diversity of Lyngbya: the new tropical marine cyanobacterial genus Dapis (Oscillatoriales). *J Phycol* **54**: 435–446.
Fabricius, K.E. (2005) Effects of terrestrial runoff on the ecology of corals and coral reefs: review and synthesis. *Mar Pollut Bull* **50**: 125–146.
Freitas, S., Hatosy, S., Fuhrman, J.A., Huse, S.M., Welch, D.B.M., Sogin, M.L., and Martiny, A.C. (2012) Global distribution and diversity of marine Verrucomicrobia. *ISME J* **6**: 1499–1505.
Frias-Lopez, J., Zerkle, A.L., Bonheyo, G.T., and Fouke, B.W. (2002) Partitioning of bacterial communities between seawater and healthy, black band diseased, and dead coral surfaces. *Appl Environ Microbiol* **68**: 2214–2228.
Fuhrman, J.A., Cram, J.A., and Needham, D.M. (2015) Marine microbial community dynamics and their ecological interpretation. *Nat Rev Microbiol* **13**: 133–146.
Gao, Y., Zhu, B., Yu, G., Chen, W., He, N., Wang, T., and Miao, C. (2014) Coupled effects of biogeochemical and hydrological processes on C, N, and P export during extreme rainfall events in a purple soil watershed in southwestern China. *J Hydrol* **511**: 692–702.
Glasl, B., Webster, N.S., and Bourne, D.G. (2017) Microbial indicators as a diagnostic tool for

717 assessing water quality and climate stress in coral reef ecosystems. *Mar Biol* **164**: 91.
718 Gloor, G.B., Macklaim, J.M., Pawlowsky-Glahn, V., and Egozcue, J.J. (2017) Microbiome
719 Datasets Are Compositional: And This Is Not Optional. *Front Microbiol* **8.**:
720 Groisman, P.Y., Knight, R.W., Easterling, D.R., Karl, T.R., Hegerl, G.C., and Razuvaev, V.N.
721 (2005) Trends in Intense Precipitation in the Climate Record. *J Clim* **18**: 1326–1350.
722 Grossmann, M.M., Gallager, S.M., and Mitarai, S. (2015) Continuous monitoring of near-bottom
723 mesoplankton communities in the East China Sea during a series of typhoons. *J Oceanogr*
724 **71**: 115–124.
725 Haapkylä, J., Unsworth, R.K.F., Flavell, M., Bourne, D.G., Schaffelke, B., and Willis, B.L. (2011)
726 Seasonal Rainfall and Runoff Promote Coral Disease on an Inshore Reef. *PLoS One* **6**:
727 e16893.
728 Harii, S., Hongo, C., Ishihara, M., Ide, Y., and Kayanne, H. (2014) Impacts of multiple
729 disturbances on coral communities at Ishigaki Island, Okinawa, Japan, during a 15 year
730 survey. *Mar Ecol Prog Ser* **509**: 171–180.
731 Hassard, F., Gwyther, C.L., Farkas, K., Andrews, A., Jones, V., Cox, B., et al. (2016)
732 Abundance and Distribution of Enteric Bacteria and Viruses in Coastal and Estuarine
733 Sediments-a Review. *Front Microbiol* **7**: 1692.
734 Hennessy, K.J., Gregory, J.M., and Mitchell, J.F.B. (1997) Changes in daily precipitation under
735 enhanced greenhouse conditions. *Clim Dyn* **13**: 667–680.
736 Herbeck, L.S., Unger, D., Krumme, U., Liu, S.M., and Jennerjahn, T.C. (2011) Typhoon-induced
737 precipitation impact on nutrient and suspended matter dynamics of a tropical estuary
738 affected by human activities in Hainan, China. *Estuar Coast Shelf Sci* **93**: 375–388.
739 Hongo, C. and Yamano, H. (2013) Species-Specific Responses of Corals to Bleaching Events
740 on Anthropogenically Turbid Reefs on Okinawa Island, Japan, over a 15-year Period
741 (1995–2009). *PLoS One* **8**: e60952.
742 Inoue, M., Ishikawa, D., Miyaji, T., Yamazaki, A., Suzuki, A., Yamano, H., et al. (2014)
743 Evaluation of Mn and Fe in coral skeletons (Porites spp.) as proxies for sediment loading
744 and reconstruction of 50 yrs of land use on Ishigaki Island, Japan. *Coral Reefs* **33**: 363–
745 373.
746 Jamieson, R., Gordon, R., Joy, D., and Lee, H. (2004) Assessing microbial pollution of rural
747 surface waters: A review of current watershed scale modeling approaches. *Agric Water*
748 *Manage* **70**: 1–17.
749 Jones, K. (2001) Campylobacters in water, sewage and the environment. *Symp Ser Soc Appl*
750 *Microbiol* 68S–79S.
751 King, A.L. and Barbeau, K.A. (2011) Dissolved iron and macronutrient distributions in the
752 southern California Current System. *J Geophys Res* **116**: 349.
753 Le, H.T., Ho, C.T., Trinh, Q.H., Trinh, D.A., Luu, M.T.N., Tran, H.S., et al. (2016) Responses of
754 Aquatic Bacteria to Terrestrial Runoff: Effects on Community Structure and Key Taxonomic
755 Groups. *Front Microbiol* **7**: 889.
756 Lewis, S.E., Schaffelke, B., Shaw, M., Bainbridge, Z.T., Rohde, K.W., Kennedy, K., et al. (2012)
757 Assessing the additive risks of PSII herbicide exposure to the Great Barrier Reef. *Mar*
758 *Pollut Bull* **65**: 280–291.
759 Lin, Y.-T., Lin, Y.-F., Tsai, I.J., Chang, E.-H., Jien, S.-H., Lin, Y.-J., and Chiu, C.-Y. (2019)
760 Structure and Diversity of Soil Bacterial Communities in Offshore Islands. *Sci Rep* **9**: 4689.
761 Loch, T.P. and Faisal, M. (2015) Emerging flavobacterial infections in fish: A review. *J Advert*
762 *Res* **6**: 283–300.
763 Love, M.I., Huber, W., and Anders, S. (2014) Moderated estimation of fold change and
764 dispersion for RNA-seq data with DESeq2. *Genome Biol* **15**: 550.
765 Masucci, G.D. and Reimer, J.D. (2019) Expanding walls and shrinking beaches: loss of natural
766 coastline in Okinawa Island, Japan. *PeerJ* **7**: e7520.
767 McMurdie, P.J. and Holmes, S. (2013) phyloseq: an R package for reproducible interactive

analysis and graphics of microbiome census data. *PLoS One* **8**: e61217.
Mei, W. and Xie, S.-P. (2016) Intensification of landfalling typhoons over the northwest Pacific since the late 1970s. *Nat Geosci* **9**: 753.
Mistri, M., Pitacco, V., Granata, T., Moruzzi, L., and Munari, C. (2019) When the levee breaks: Effects of flood on offshore water contamination and benthic community in the Mediterranean (Ionian Sea). *Mar Pollut Bull* **140**: 588–596.
Munro, P.M., Gauthier, M.J., Breittmayer, V.A., and Bongiovanni, J. (1989) Influence of osmoregulation processes on starvation survival of Escherichia coli in seawater. *Appl Environ Microbiol* **55**: 2017–2024.
O'Connor, J.J., Lecchini, D., Beck, H.J., Cadiou, G., Lecellier, G., Booth, D.J., and Nakamura, Y. (2016) Sediment pollution impacts sensory ability and performance of settling coral-reef fish. *Oecologia* **180**: 11–21.
Oksanen, J., Guillaume Blanchet, F., Friendly, M., Kindt, R., Legendre, P., McGlinn, D., et al. (2019) vegan: Community Ecology Package. R package version 2.5-4.
Omija, T. (2004) Terrestrial inflow of soils and nutrients. *Coral Reefs of Japan* **47**: 64–68.
Omori, M. (2011) Degradation and restoration of coral reefs: Experience in Okinawa, Japan. *Mar Biol Res* **7**: 3–12.
Paerl, H.W., Bales, J.D., Ausley, L.W., Buzzelli, C.P., Crowder, L.B., Eby, L.A., et al. (2001) Ecosystem impacts of three sequential hurricanes (Dennis, Floyd, and Irene) on the United States' largest lagoonal estuary, Pamlico Sound, NC. *Proc Natl Acad Sci U S A* **98**: 5655–5660.
Paerl, H.W., Crosswell, J.R., Van Dam, B., Hall, N.S., Rossignol, K.L., Osburn, C.L., et al. (2018) Two decades of tropical cyclone impacts on North Carolina's estuarine carbon, nutrient and phytoplankton dynamics: implications for biogeochemical cycling and water quality in a stormier world. *Biogeochemistry* **141**: 307–332.
Paerl, H.W., Valdes, L.M., Joyner, A.R., Peierls, B.L., Piehler, M.F., Riggs, S.R., et al. (2006) Ecological response to hurricane events in the Pamlico Sound system, North Carolina, and implications for assessment and management in a regime of increased frequency. *Estuaries Coasts* **29**: 1033–1045.
Pandey, P.K., Kass, P.H., Soupir, M.L., Biswas, S., and Singh, V.P. (2014) Contamination of water resources by pathogenic bacteria. *AMB Express* **4**: 51.
Patterson, K.L., Porter, J.W., Ritchie, K.B., Polson, S.W., Mueller, E., Peters, E.C., et al. (2002) The etiology of white pox, a lethal disease of the Caribbean elkhorn coral, Acropora palmata. *Proc Natl Acad Sci U S A* **99**: 8725–8730.
Pearman, J.K., Afandi, F., Hong, P., and Carvalho, S. (2018) Plankton community assessment in anthropogenic-impacted oligotrophic coastal regions. *Environ Sci Pollut Res Int* **25**: 31017–31030.
Perrone, J. and Madramootoo, C.A. (1998) Improved curve number selection for runoff prediction. *Can J Civ Eng* **25**: 728–734.
Peters, E.C. (2015) Diseases of Coral Reef Organisms. In *Coral Reefs in the Anthropocene*. Birkeland, C. (ed). Dordrecht: Springer Netherlands, pp. 147–178.
Philipp, E. and Fabricius, K. (2003) Photophysiological stress in scleractinian corals in response to short-term sedimentation. *J Exp Mar Bio Ecol* **287**: 57–78.
Pollock, F.J., Lamb, J.B., Field, S.N., Heron, S.F., Schaffelke, B., Shedrawi, G., et al. (2014) Sediment and turbidity associated with offshore dredging increase coral disease prevalence on nearby reefs. *PLoS One* **9**: e102498.
Pruzzo, C., Huq, A., Colwell, R.R., and Donelli, G. (2005) Pathogenic Vibrio Species in the Marine and Estuarine Environment. In *Oceans and Health: Pathogens in the Marine Environment*. Belkin, S. and Colwell, R.R. (eds). Boston, MA: Springer US, pp. 217–252.
Quast, C., Pruesse, E., Yilmaz, P., Gerken, J., Schweer, T., Yarza, P., et al. (2013) The SILVA ribosomal RNA gene database project: improved data processing and web-based tools.

Nucleic Acids Res **41**: D590–6.
Riegl, B. and Branch, G.M. (1995) Effects of sediment on the energy budgets of four scleractinian (Bourne 1900) and five alcyonacean (Lamouroux 1816) corals. *J Exp Mar Bio Ecol* **186**: 259–275.
Sañudo-Wilhelmy, S.A., Kustka, A.B., Gobler, C.J., Hutchins, D.A., Yang, M., Lwiza, K., et al. (2001) Phosphorus limitation of nitrogen fixation by Trichodesmium in the central Atlantic Ocean. *Nature* **411**: 66–69.
Sharma, S., Sachdeva, P., and Virdi, J.S. (2003) Emerging water-borne pathogens. *Appl Microbiol Biotechnol* **61**: 424–428.
Sheridan, C., Baele, J.M., Kushmaro, A., Fréjaville, Y., and Eeckhaut, I. (2014) Terrestrial runoff influences white syndrome prevalence in SW Madagascar. *Mar Environ Res* **101**: 44–51.
Shinn, E.A., Smith, G.W., Prospero, J.M., Betzer, P., Hayes, M.L., Garrison, V., and Barber, R.T. (2000) African dust and the demise of Caribbean Coral Reefs. *Geophys Res Lett* **27**: 3029–3032.
Siegesmund, M.A., Johansen, J.R., Karsten, U., and Friedl, T. (2008) COLEOFASCICULUS GEN. NOV. (CYANOBACTERIA): MORPHOLOGICAL AND MOLECULAR CRITERIA FOR REVISION OF THE GENUS MICROCOLEUS GOMONT(1). *J Phycol* **44**: 1572–1585.
Silva, J., Leite, D., Fernandes, M., Mena, C., Gibbs, P.A., and Teixeira, P. (2011) Campylobacter spp. as a Foodborne Pathogen: A Review. *Front Microbiol* **2**: 200.
Solo-Gabriele, H.M., Wolfert, M.A., Desmarais, T.R., and Palmer, C.J. (2000) Sources of Escherichia coli in a coastal subtropical environment. *Appl Environ Microbiol* **66**: 230–237.
Soo, R.M., Skennerton, C.T., Sekiguchi, Y., Imelfort, M., Paech, S.J., Dennis, P.G., et al. (2014) An expanded genomic representation of the phylum cyanobacteria. *Genome Biol Evol* **6**: 1031–1045.
Sussman, M., Willis, B.L., Victor, S., and Bourne, D.G. (2008) Coral Pathogens Identified for White Syndrome (WS) Epizootics in the Indo-Pacific. *PLoS One* **3**: e2393.
Sutherland, K.P., Porter, J.W., and Torres, C. (2004) Disease and immunity in Caribbean and Indo-Pacific zooxanthellate corals. *Mar Ecol Prog Ser* **266**: 273–302.
Sutherland, K.P., Shaban, S., Joyner, J.L., Porter, J.W., and Lipp, E.K. (2011) Human pathogen shown to cause disease in the threatened eklhorn coral Acropora palmata. *PLoS One* **6**: e23468.
Vizcaino, M.I., Johnson, W.R., Kimes, N.E., Williams, K., Torralba, M., Nelson, K.E., et al. (2010) Antimicrobial resistance of the coral pathogen Vibrio coralliilyticus and Caribbean sister phylotypes isolated from a diseased octocoral. *Microb Ecol* **59**: 646–657.
Voss, J.D. and Richardson, L.L. (2006) Coral diseases near Lee Stocking Island, Bahamas: patterns and potential drivers. *Dis Aquat Organ* **69**: 33–40.
Wang, B., Yang, Y., Ding, Q.-H., Murakami, H., and Huang, F. (2010) Climate control of the global tropical storm days (1965-2008): CLIMATE CONTROL OF TROPICAL STORM DAYS. *Geophys Res Lett* **37.**:
Weber, M., de Beer, D., Lott, C., Polerecky, L., Kohls, K., Abed, R.M.M., et al. (2012) Mechanisms of damage to corals exposed to sedimentation. *Proc Natl Acad Sci U S A* **109**: E1558–67.
Weiskel, P.K., Howes, B.L., and Heufelder, G.R. (1996) Coliform Contamination of a Coastal Embayment: Sources and Transport Pathways. *Environ Sci Technol* **30**: 1872–1881.
Wetz, M.S. and Paerl, H.W. (2008) Estuarine Phytoplankton Responses to Hurricanes and Tropical Storms with Different Characteristics (Trajectory, Rainfall, Winds). *Estuaries Coasts* **31**: 419–429.
Willis, A. and Bunge, J. (2015) Estimating diversity via frequency ratios. *Biometrics* **71**: 1042–1049.
Willis, A., Bunge, J., and Whitman, T. (2017) Improved detection of changes in species richness in high diversity microbial communities. *J R Stat Soc C* **66**: 963–977.

Wilson, B., Aeby, G.S., Work, T.M., and Bourne, D.G. (2012) Bacterial communities associated with healthy and Acropora white syndrome-affected corals from American Samoa. *FEMS Microbiol Ecol* **80**: 509–520.
Witt, V., Wild, C., and Uthicke, S. (2012) Terrestrial runoff controls the bacterial community composition of biofilms along a water quality gradient in the Great Barrier Reef. *Appl Environ Microbiol* **78**: 7786–7791.
Wooldridge, S.A. (2009) Water quality and coral bleaching thresholds: formalising the linkage for the inshore reefs of the Great Barrier Reef, Australia. *Mar Pollut Bull* **58**: 745–751.
Wu, J. and Boyle, E.A. (1998) Determination of iron in seawater by high-resolution isotope dilution inductively coupled plasma mass spectrometry after Mg(OH)2 coprecipitation. *Anal Chim Acta* **367**: 183–191.
Wu, J., Chung, S.-W., Wen, L.-S., Liu, K.-K., Chen, Y.-L.L., Chen, H.-Y., and Karl, D.M. (2003) Dissolved inorganic phosphorus, dissolved iron, and Trichodesmium in the oligotrophic South China Sea : PHOSPHATE, IRON, AND NITROGEN FIXATION IN THE SOUTH CHINA SEA. *Global Biogeochem Cycles* **17**: 8–1–8–10.
Yamano, H. and Watanabe, T. (2016) Coupling Remote Sensing and Coral Annual Band Data to Investigate the History of Catchment Land Use and Coral Reef Status. In *Coral Reef Science: Strategy for Ecosystem Symbiosis and Coexistence with Humans under Multiple Stresses*. Kayanne, H. (ed). Tokyo: Springer Japan, pp. 47–53.
Yamazaki, A., Watanabe, T., Tsunogai, U., Hasegawa, H., and Yamano, H. (2015) The coral δ15N record of terrestrial nitrate loading varies with river catchment land use. *Coral Reefs*.
Yeo, S.K., Huggett, M.J., Eiler, A., and Rappé, M.S. (2013) Coastal bacterioplankton community dynamics in response to a natural disturbance. *PLoS One* **8**: e56207.
Zhang, J.-Z., Kelble, C.R., Fischer, C.J., and Moore, L. (2009) Hurricane Katrina induced nutrient runoff from an agricultural area to coastal waters in Biscayne Bay, Florida. *Estuar Coast Shelf Sci* **84**: 209–218.
Zhou, W., Yin, K., Harrison, P.J., and Lee, J.H.W. (2012) The influence of late summer typhoons and high river discharge on water quality in Hong Kong waters. *Estuar Coast Shelf Sci* **111**: 35–47.
Zimmer, B.L., May, A.L., Bhedi, C.D., Dearth, S.P., Prevatte, C.W., Pratte, Z., et al. (2014) Quorum sensing signal production and microbial interactions in a polymicrobial disease of corals and the coral surface mucopolysaccharide layer. *PLoS One* **9**: e108541.

R Core Team (2018). R: A language and environment for statistical computing. R Foundation for Statistical Computing, Vienna, Austria. URL https://www.R-project.org/.

Figure legends

Figure 1. Location of the study area A) Map locating Okinawa Island in the East China Sea. B) Map showing the location of the central-west coast of Okinawa Island. C) Location of the 4 nearshore sampling points in Onna-son, on the central-west coast of Okinawa Island.

Figure 2. Precipitation (in mm day^{-1}) and wind speed (m s^{-1}) during the 2018 typhoon season in Okinawa, Japan. Data were collected with the meteorological station located at OIST Marine Science Station (26.510046 ˚N, 127.871721 ˚E) from June through October, corresponding to the duration of the typhoon season in Okinawa. Bars represent the daily amount of rain (in mm); dashed black and red lines indicate daily mean and maximum wind speeds (in m s^{-1}); shaded areas represent the two red soil pollution events monitored in this study: Tropical Storm Gaemi on June 16 and the super-typhoons Trami and Kong-Rey on September 29 and October 5. The dates when water samples were collected for chemical and DNA analyses are noted on the x-axis.

Figure 3. Temporal variation of physicochemical parameters before, during, and after storm events in June and October, 2018. Bars represent the values of temperature (°C), turbidity (NTU), salinity (‰) and concentrations of micro- and macro-nutrient concentrations (NO_2^-, NO_3^-, NH_4^+, PO_4^{3-}, SiO_2 in µM; dFe in nM) at sampling sites A1–4 along the central west coast of Okinawa, Japan. Error bars represent one standard deviation of the mean from four replicates. Red dashed vertical lines represent the timing of major storms and associated red soil pollution events. Sampling dates when samples were also processed for metabarcode analyses are indicated in bold on the x-axis. Temperature (°C), turbidity (NTU) and salinity (‰) measurements were taken with a CTD probe. Macro-nutrient concentrations were determined on a QuAAtro39 Continuous Segmented Flow Analyzer and dFe concentration was determined by ICP-MS after $Mg(OH)_2$ co-precipitation using the isotope dilution method(Wu and Boyle, 1998).

Figure 4. Relative abundance of bacterial phyla in field and mesocosm samples collected in June and October, 2018. Each stacked bar represents the relative contribution of major bacterial phyla to the total community at one sampling location, in one red soil sample, or at one time point in mesocosms (mesocosm bars represent aggregate data from 4–5 replicates depending on month and treatment). Sampling stations (A)1–4 were sampled before, during, and after major storms affecting Okinawa in June and October 2018. In June, the storm affected Okinawa on 6/16, so that sampling on 6/13 was before the storm and sampling on 6/19 was afterward. In October, two super typhoons affected Okinawa on 9/28 and 10/05 so that 9/28 was before the event window, 10/01 and 10/03 was during the event window, and 10/08 was afterward. Red soil samples are labeled with replicate numbers and were collected within a week of the storms in June and October. Red soil (200 mg L^{-1}) was added to treatment mesocosms immediately following the t0 sampling.

Figure 5. Principal component analysis (PCA) of Aitchison distances between bacterial community composition before, during, and after storm events in June (A) and October (B), 2018. (A) June 13 was before the June storm, 6/16 was during, and 6/19 was after. For the October storms (B), 9/28 was before the storms, 10/01 and 10/03 were between, and 10/08 was after. Samples collected during/between storm events separate from samples collected before and after storms on PC1 for both the June and October events.

Figure 6. Richness estimates for bacterial communities in red soil samples and surface water samples collected before, during, and after storm events in June (A) and October (B), 2018. Red dashed vertical lines represent the timing

of major storms. In June (A), the red soil samples had significantly higher richness than the water samples collected before and after the storm, but not samples collected during the storm. In October (B), red soil samples had significantly higher richness than all water samples and richness was not significantly different in water samples collected before, during, or after the storms. Differences in richness were considered significant when $p < 0.05$.

Figure 7. Number of Amplicon Sequence Variants (ASVs) significantly differentially abundant in pairwise comparisons between sampling dates in June (A) and October (C) and log2 Fold Change of individual ASVs in pairwise comparisons from before to during storms and from before to after storms in June (B) and October (D), 2018. ASVs were considered significantly differentially abundant when the FDR adjusted *p*-value was less than 0.05. ASVs that were also present in soil samples are colored red in panels A and B; no differentially abundant ASVs in pairwise tests for October samples were found to be present in October soil samples. Positive log2FoldChange values (x-axis, B, D) indicate higher abundance of ASVs during/between storms compared to before (J13 to J16, S28 to O01 + O03) or after storms compared to before (J13 to J19, S28 to O08). Differentially abundant ASVs are grouped by taxonomic order and orders are color coded by phylum so that colors correspond to Figure 4.

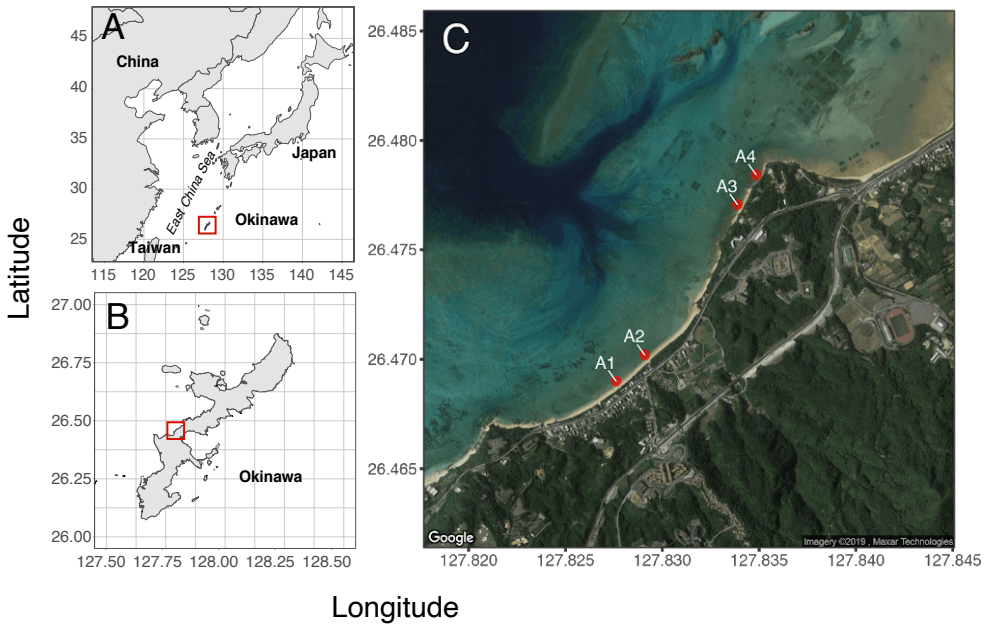
A
China
Japan
East China Sea
Okinawa
Taiwan
45
40
35
30
25
115 120 125 130 135 140 145
B
Okinawa
27.00
26.75
26.50
26.25
26.00
127.50 127.75 128.00 128.25 128.50
C
A4
A3
A2
A1
26.485
26.480
26.475
26.470
26.465
Google
Imagery ©2019 , Maxar Technologies
127.820 127.825 127.830 127.835 127.840 127.845
Latitude
Longitude

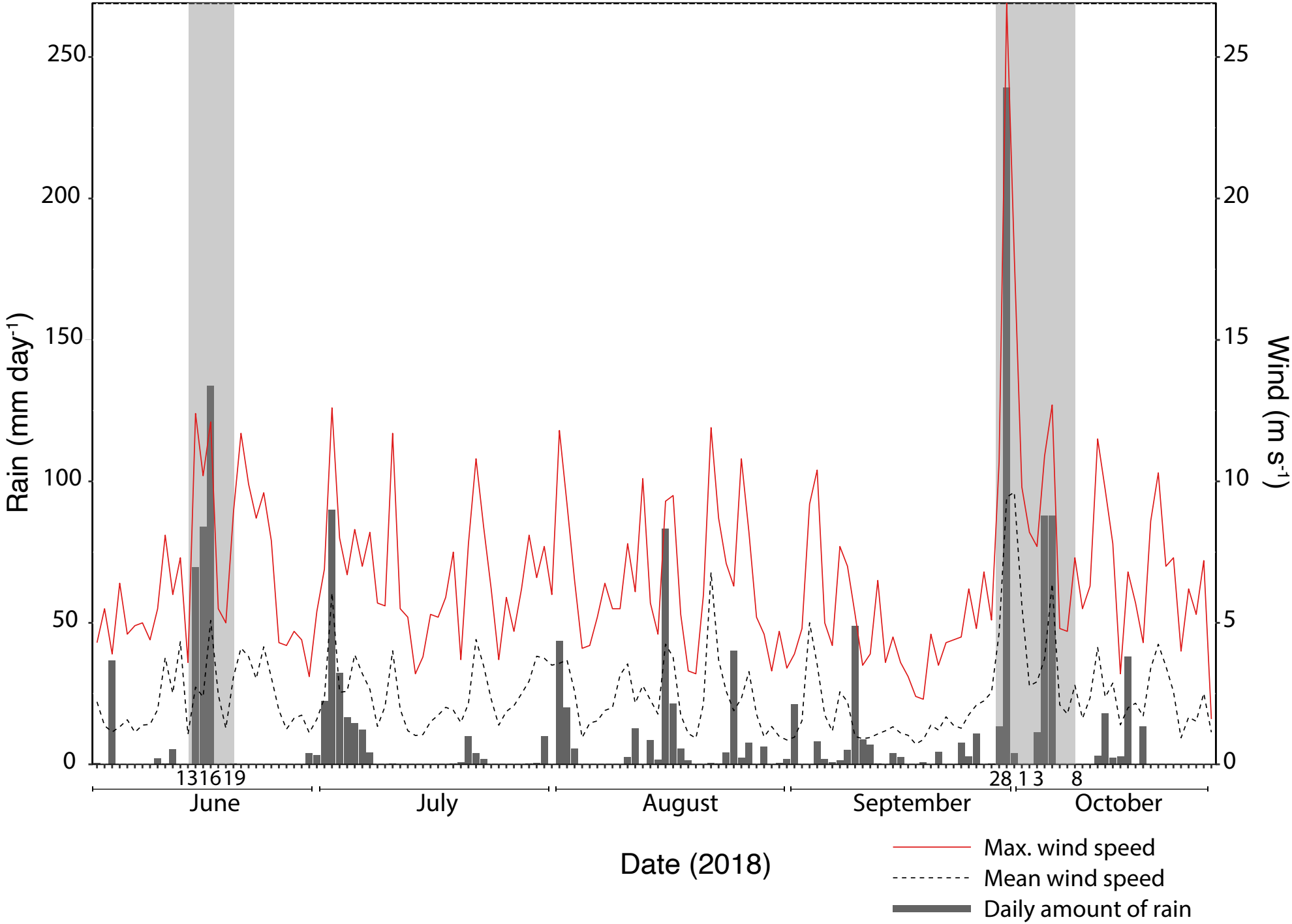
Rain (mm day-1)
Wind (m s-1)
250
200
150
100
50
0
25
20
15
10
5
0
13
16
19
28
1
3
8
June
July
August
September
October
Date (2018)
Max. wind speed
Mean wind speed
Daily amount of rain

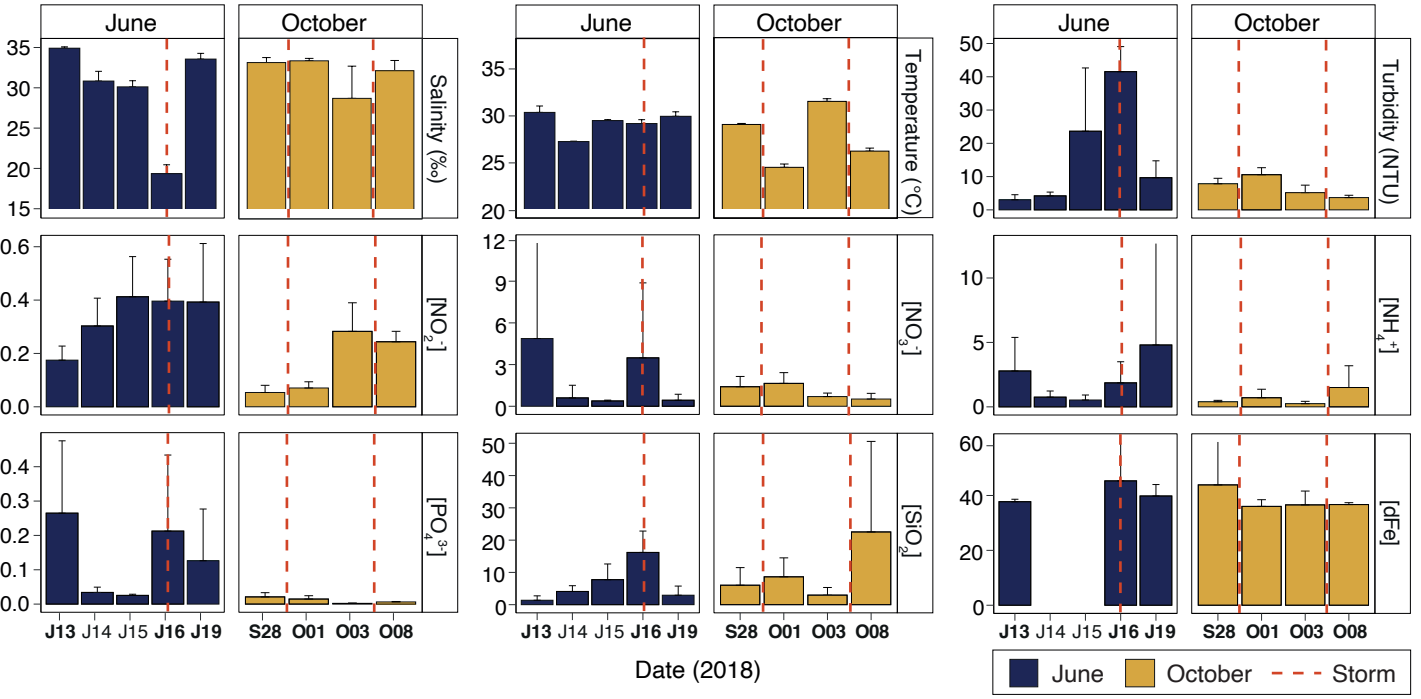
June
October
Salinity (‰)
Temperature (°C)
Turbidity (NTU)
[NO2-]
[NO3-]
[NH4+]
[PO4 3-]
[SiO2]
[dFe]
J13 J14 J15 J16 J19
S28 O01 O03 O08
Date (2018)
June
October
Storm

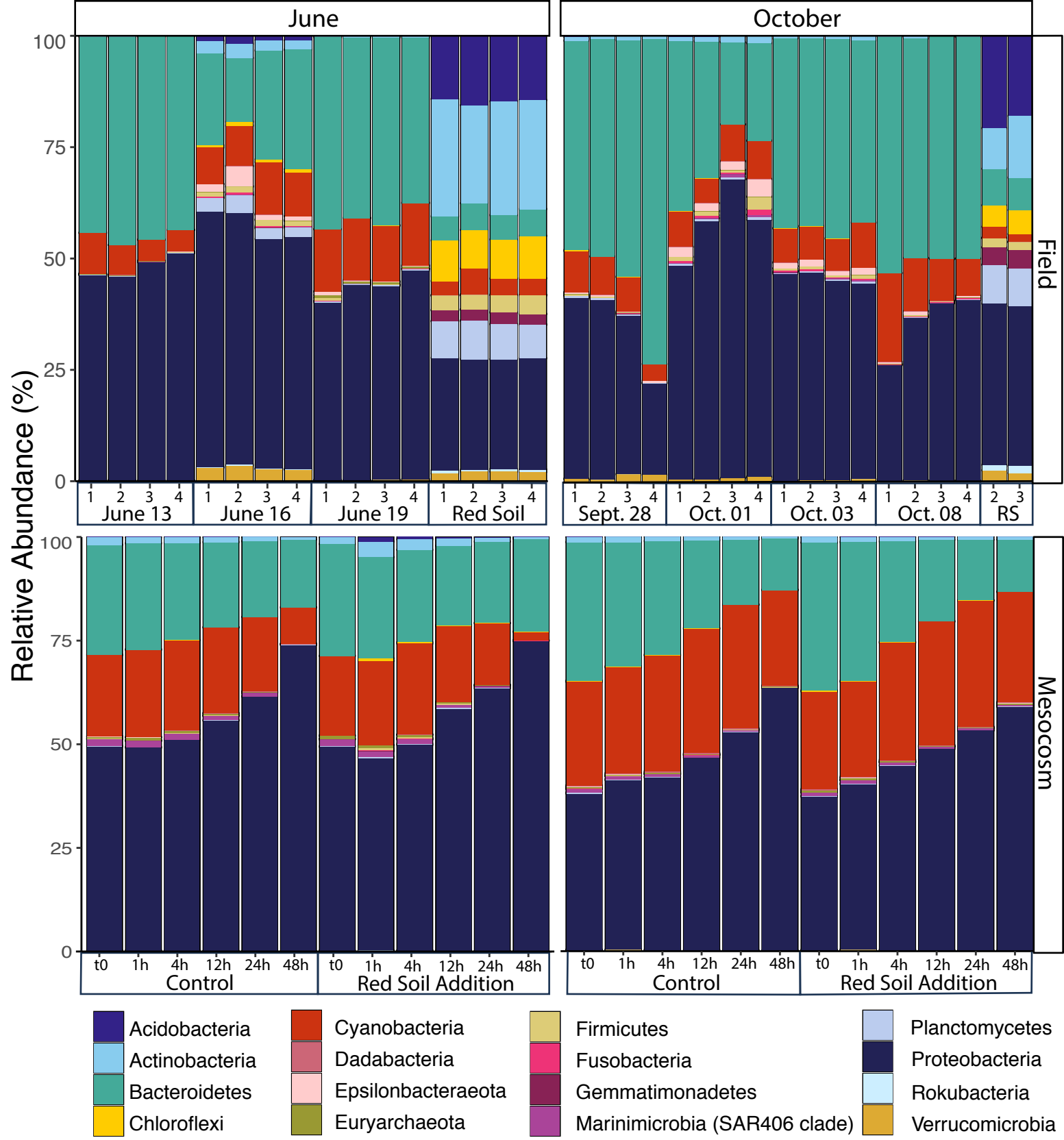
June
October
Field
Mesocosm
Relative Abundance (%)
100
75
50
25
0
1 2 3 4
June 13
June 16
June 19
Red Soil
Sept. 28
Oct. 01
Oct. 03
Oct. 08
RS
2 3
t0 1h 4h 12h 24h 48h
Control
Red Soil Addition
Acidobacteria
Actinobacteria
Bacteroidetes
Chloroflexi
Cyanobacteria
Dadabacteria
Epsilonbacteraeota
Euryarchaeota
Firmicutes
Fusobacteria
Gemmatimonadetes
Marinimicrobia (SAR406 clade)
Planctomycetes
Proteobacteria
Rokubacteria
Verrucomicrobia

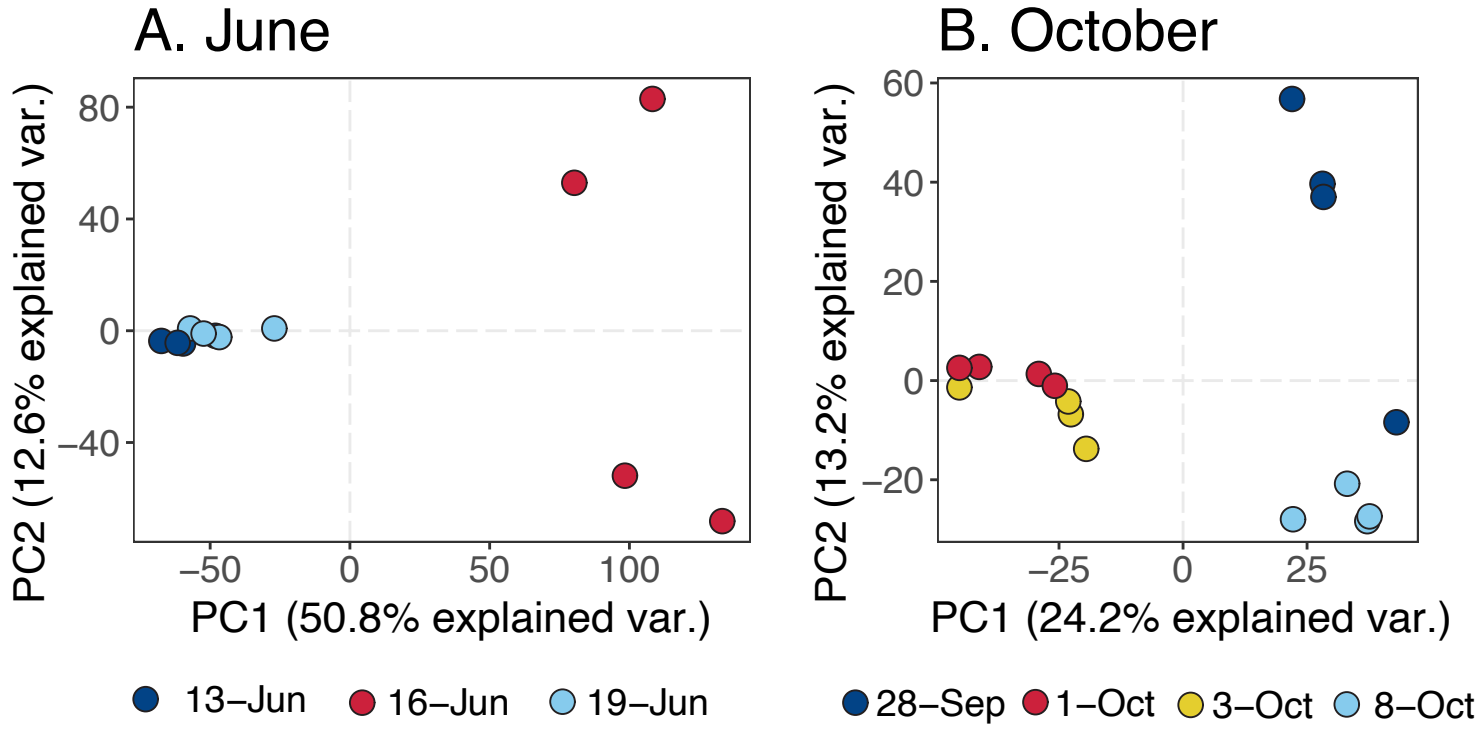
A. June
B. October
PC2 (12.6% explained var.)
PC1 (50.8% explained var.)
PC2 (13.2% explained var.)
PC1 (24.2% explained var.)
80
40
0
−40
−50
0
50
100
60
40
20
0
−20
−25
0
25
13−Jun
16−Jun
19−Jun
28−Sep
1−Oct
3−Oct
8−Oct

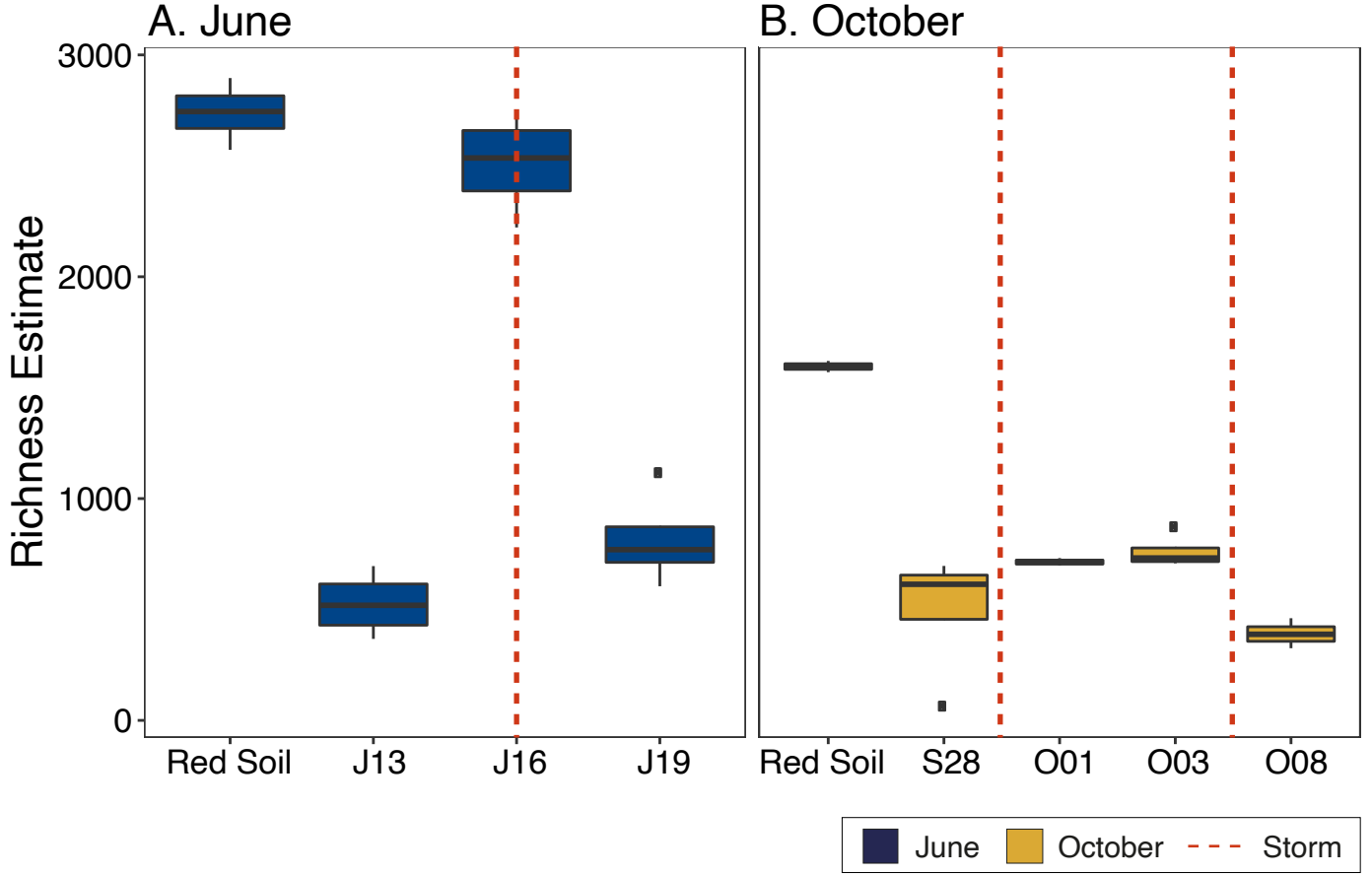
A. June
B. October
Richness Estimate
3000
2000
1000
0
Red Soil
J13
J16
J19
Red Soil
S28
O01
O03
O08
June
October
Storm

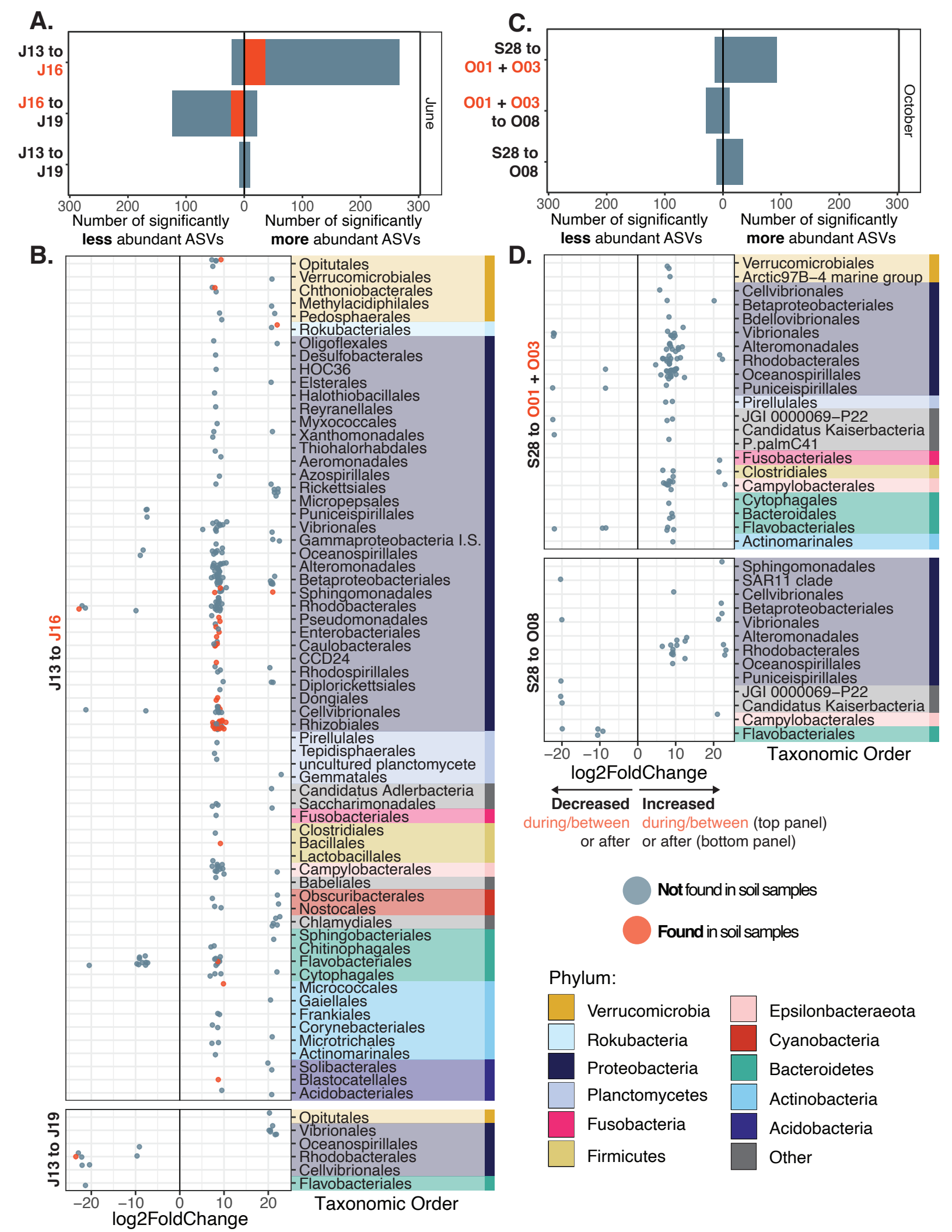
A.
J13 to J16
J16 to J19
J13 to J19
June
300 200 100 0 100 200 300
Number of significantly less abundant ASVs
Number of significantly more abundant ASVs
C.
S28 to O01 + O03
O01 + O03 to O08
S28 to O08
October
300 200 100 0 100 200 300
Number of significantly less abundant ASVs
Number of significantly more abundant ASVs
B.
J13 to J16
Opitutales
Verrucomicrobiales
Chthoniobacterales
Methylacidiphilales
Pedosphaerales
Rokubacteriales
Oligoflexales
Desulfobacterales
HOC36
Elsterales
Halothiobacillales
Reyranellales
Myxococcales
Xanthomonadales
Thiohalorhabdales
Aeromonadales
Azospirillales
Rickettsiales
Micropepsales
Puniceispirillales
Vibrionales
Gammaproteobacteria I.S.
Oceanospirillales
Alteromonadales
Betaproteobacteriales
Sphingomonadales
Rhodobacterales
Pseudomonadales
Enterobacteriales
Caulobacterales
CCD24
Rhodospirillales
Diplorickettsiales
Dongiales
Cellvibrionales
Rhizobiales
Pirellulales
Tepidisphaerales
uncultured planctomycete
Gemmatales
Candidatus Adlerbacteria
Saccharimonadales
Fusobacteriales
Clostridiales
Bacillales
Lactobacillales
Campylobacterales
Babeliales
Obscuribacterales
Nostocales
Chlamydiales
Sphingobacteriales
Chitinophagales
Flavobacteriales
Cytophagales
Micrococcales
Gaiellales
Frankiales
Corynebacteriales
Microtrichales
Actinomarinales
Solibacterales
Blastocatellales
Acidobacteriales
J13 to J19
Opitutales
Vibrionales
Oceanospirillales
Rhodobacterales
Cellvibrionales
Flavobacteriales
−20 −10 0 10 20
log2FoldChange
Taxonomic Order
D.
S28 to O01 + O03
Verrucomicrobiales
Arctic97B−4 marine group
Cellvibrionales
Betaproteobacteriales
Bdellovibrionales
Vibrionales
Alteromonadales
Rhodobacterales
Oceanospirillales
Puniceispirillales
Pirellulales
JGI 0000069−P22
Candidatus Kaiserbacteria
P.palmC41
Fusobacteriales
Clostridiales
Campylobacterales
Cytophagales
Bacteroidales
Flavobacteriales
Actinomarinales
S28 to O08
Sphingomonadales
SAR11 clade
Cellvibrionales
Betaproteobacteriales
Vibrionales
Alteromonadales
Rhodobacterales
Oceanospirillales
Puniceispirillales
JGI 0000069−P22
Candidatus Kaiserbacteria
Campylobacterales
Flavobacteriales
−20 −10 0 10 20
log2FoldChange
Taxonomic Order
Decreased during/between or after
Increased during/between (top panel) or after (bottom panel)
Not found in soil samples
Found in soil samples
Phylum:
Verrucomicrobia
Rokubacteria
Proteobacteria
Planctomycetes
Fusobacteria
Firmicutes
Epsilonbacteraeota
Cyanobacteria
Bacteroidetes
Actinobacteria
Acidobacteria
Other